Applied Geochemistry 28 (2013) 164–171

Contents lists available at SciVerse ScienceDirect

Applied Geochemistry

journal homepage: www.elsevier.com/locate/apgeochem

Influence of a summer storm event on the flux and composition of dissolved organic matter in a subtropical river, China

Liyang Yang, Weidong Guo, Nengwang Chen, Huasheng Hong *, Jinliang Huang, Jing Xu, Shuiying Huang

State Key Laboratory of Marine Environmental Science, College of Oceanography and Environmental Science, Xiamen University, Xiamen 361005, PR China

ARTICLE INFO

Article history:
Received 24 April 2012
Accepted 5 October 2012
Available online 15 October 2012
Editorial handling by M. Kersten

ABSTRACT

Dissolved organic matter (DOM) has not been studied fully for tropical and subtropical rivers, in particular during storm events. DOM dynamics during a summer storm event in June, 2011 were examined in a subtropical river (the North Jiulong River, China). Stormwater runoff was sampled for measurement of dissolved organic C (DOC), absorption spectroscopy and fluorescence excitation emission matrix spectroscopy (EEMs). Three different fluorescent components were identified using parallel factor analysis (PARAFAC), including humic-like C1 and C3, and C2 as a combination of humic-like and protein-like fluorophores. The flux of DOC increased fivefold from 0.4 kg s^{-1} at baseflow to 2.0 kg s^{-1} at peak flow. Chromophoric DOM (CDOM) and fluorescent components also showed large increases with stormflow. The flux of DOC was similar during the rising and falling hydrographs at equal water discharge, while those of CDOM and fluorescent components were much higher during the falling-hydrograph. Carbon specific CDOM absorption coefficient at UV ($SUVA_{254}$) and the fraction of C3 which fluoresced at long emission wavelength correlated positively to each other but negatively to absorption spectral slope ratio (S_R) and C2%. They showed notable temporal variations indicative of increases in aromaticity, C3% and average molecular weight of DOM during the storm event. Changes in DOM composition lagged behind those in DOM flux. Changes in the flux and quality of DOM during the storm event, which were monitored effectively by absorption spectroscopy and EEMs–PARAFAC, could affect biogeochemical processes in the river and receiving coastal waters.

1. Introduction

Dissolved organic matter (DOM) is the largest pool of reduced C and plays important roles in a variety of biogeochemical processes and ecosystem function in aquatic environments (Benner, 2003). For example, abundant C and nutrient elements (such as N and P) are bound within DOM, which can be released as CO_2 and bioavailable inorganic nutrients upon the decomposition of DOM (e.g., Moran and Zepp, 1997; Stedmon et al., 2007; Lonborg and Sondergaard, 2009). The speciation, solubility, bioavailability and toxicity of metals are also affected by DOM (e.g., Sánchez-Marín et al., 2010; Hassler et al., 2011). The microbial utilization of DOM is the start of the microbial food loop, while the microbial transformation of labile DOM to refractory DOM can store C for thousands of years in the ocean (Jiao et al., 2010). Chromophoric DOM (CDOM), which absorbs both photosynthetically active and ultraviolet radiation, affects both primary production and the habitat for organisms (Coble, 2007). The biogeochemical reactivity of DOM is largely dependent on its chemical composition. For example, the bioavailability of DOM is related to its molecular weight (Loh et al., 2004) and the fraction of protein-like materials (Fellman et al., 2009, 2010). Different constituents of DOM have variable photochemical reactivity (Kieber et al., 2007; Spencer et al., 2009; Stubbins et al., 2010). Therefore, to better understand the biogeochemical role of DOM, it is important to examine both the concentration and composition of DOM in aquatic environments.

Annually, approximately 0.2–0.25 Gt C in DOM is transported by global rivers to the ocean (Ludwig et al., 1996; Battin et al., 2008), which represents an important biogeochemical linkage between the terrestrial and marine ecosystems. Recent studies have focused disproportionately on temperate and high-latitude rivers, but tropical rivers contribute more to the global land–ocean flux of dissolved organic C (DOC) (Spencer et al., 2010; Ludwig et al., 1996). In addition, our understanding of DOM dynamics in tropical rivers is largely limited to a few large systems (e.g. Mayorga et al., 2005; He et al., 2010), and the factors that control the concentration, composition and flux of DOM in many other medium-sized and small rivers require further study. In fact, the biogeochemistry of DOM in rivers can be affected significantly by many factors such as hydrological condition, geological settings, land use, microbial activity and photo-degradation (e.g. Hood et al., 2006; Williams et al., 2010; Yamashita et al., 2010, 2011; Cawley et al., 2012; Hong et al., 2012).

* Corresponding author. Tel.: +86 592 2182216; fax: +86 592 2095242.
E-mail address: hshong@xmu.edu.cn (H. Hong).

0883-2927/$ - see front matter © 2012 Elsevier Ltd. All rights reserved.
http://dx.doi.org/10.1016/j.apgeochem.2012.10.004

In particular, the concentration, composition and flux of DOM can change greatly during storm events. For example, the DOC concentration increases by approximately threefold and the proportion of humic DOM was shown to increase in a storm event in three small watersheds in Oregon (Hood et al., 2006). The mean concentration and flux of DOC at stormflow are 2.2 and 57 times higher than those at baseflow in the Wailuku River, Hawaii (Wiegner et al., 2009). Storm and snow melt events together accounts for ~86% of DOC export in 30 small forested watersheds in the eastern USA, and one critical area of future research is to study compositional changes of DOM during these events (Raymond and Saiers, 2010). The protein-like fraction in total fluorescence and the bioavailability of DOM decrease in an upland watershed but increase in a wetland dominated watershed during stormflows in Alaskan Rivers (Fellman et al., 2009). To better evaluate the biogeochemical role of DOM in linking the terrestrial and marine ecosystems, it is important to study the flux and composition of DOM during storm events, in particular considering that most studies have focused on DOM under baseflow conditions and that the frequency of heavy precipitation events is likely to increase in the future due to climate change (IPCC, 2007).

Absorption and fluorescence spectroscopy are useful for characterizing the concentration and composition of DOM. Absorption coefficient and fluorescence intensity are indicators for the levels of CDOM and fluorophores, while the carbon specific CDOM absorption coefficient at UV ($SUVA_{254}$), and absorption spectral slope ratio (S_R) are valuable proxies for the composition of DOM (Weishaar et al., 2003; Helms et al., 2008). Fluorescence excitation emission matrix spectroscopy coupled with parallel factor analysis (EEMs–PARAFAC) provides a powerful tool for differentiating fluorescent components and tracing their dynamics (e.g., Stedmon and Markager, 2005; Kowalczuk et al., 2009; Fellman et al., 2010; Chen et al., 2010; Yang et al., 2012a; Maie et al., 2012). Only recently have a very few studies applied fluorescence spectroscopy to study DOM dynamics in storm events and they were limited to mid-high latitude rivers (Fellman et al., 2009; Austnes et al., 2010; Nguyen et al., 2010). Studies are required to assess the potential of such techniques with respect to DOM dynamics in tropical watersheds.

The Jiulong River is a subtropical river located in southeastern China, with distinct dry and wet seasons under the influence of the East Asian Monsoon. Tropical storms violently impact this area several times per year and bring heavy precipitation, which may lead to rapid flushing of DOM from the land to the ocean. The effects of storm events on the level and composition of DOM is poorly studied for not only the Jiulong River but also many other rivers in this region including some large ones such as the Yangtze River and the Pearl River (Fig. 1). Although a higher DOM concentration and a lower protein-like fraction in total fluorescence have been observed after storms than in the dry season in the authors' five basin scale investigations (Hong et al., 2012), the dynamics of DOM at high temporal resolution in a storm event with changing flow is unknown. This study aimed to examine the temporal changes in the flux and composition of DOM in a summer storm event, using DOC, absorption spectroscopy and EEMs–PARAFAC.

2. Materials and methods

2.1. Study area

The Jiulong River is a subtropical river located in Fujian province, southeastern China, with a drainage area of 14,741 km^2. The mean annual temperature and precipitation are 19.9–21.1 °C and 1400–1800 mm. The main land cover of the watershed is forestland (69.4%) and arable land (18.4%) (Huang et al., 2011). There are three major tributaries in the watershed: North River, West River and South River (Fig. 1). The North River is the main tributary with a length of 274 km, a drainage area of 9803 km^2 (accounting for 66.5% of the total area of the Jiulong River watershed) and a mean annual discharge of 82.3×10^8 m^3 (with ~74% occurring in the wet season from April to September).

2.2. Field sampling

A summer storm event occurred in the North Jiulong River watershed from 23:00, June 11 to 17:00, June 12, 2011 (Fig. 2), with a mean rainfall of 64.25 mm at the four weather stations (Fig. 1) and a highest one of 143 mm at the upstream site (Longyan). In addition, there were two moderate rains on June 11 and 14. The water discharge at the most downstream hydrological station Punan increased strongly from 214 $m^3\ s^{-1}$ on June 11 to a maximum value of 1000 $m^3\ s^{-1}$ on June 13, mainly due to the storm event and

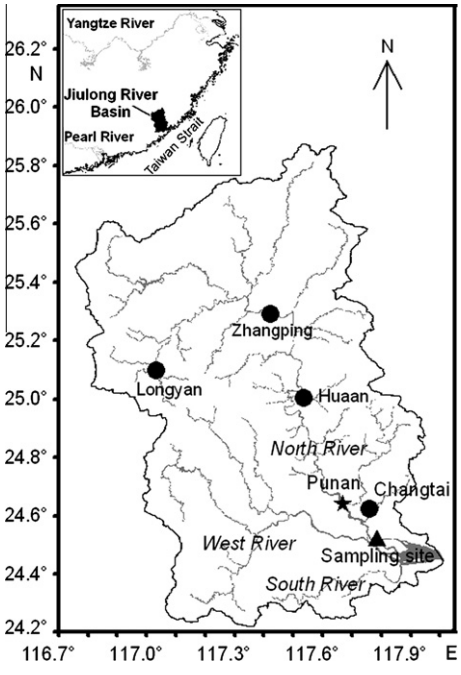

Fig. 1. Study area, sampling site (triangle), the most downriver hydrological station (star: Punan) and the four weather stations (circle: Longyan, Zhangping, Huaan and Changtai) in the North Jiulong River.

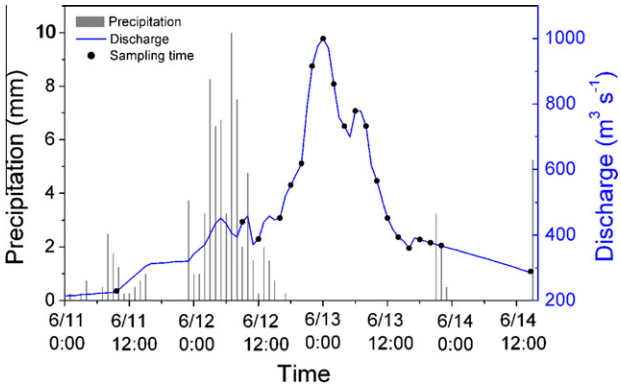

Fig. 2. Changes in mean precipitation at four locations in the North Jiulong River and the water discharge at Punan gauge during the storm event in June, 2011. Hourly rainfall data are from the Fujian Water Information system, http://www.fjwater.gov.cn/; Hourly flow rate was provided by Punan gauge, Fujian Province.

partly to the moderate rain on June 11 (Figs. 1 and 2). The flow peak lagged the maximum precipitation by 18 h, which represented the time for the water to flow from the land into the river channel and from upstream to downriver. After the flow peak at 0:00 on June 13, the discharge generally decreased to 289 $m^3 s^{-1}$ at 14:47 on June 14 (i.e. the end of the observation).

Surface runoff was collected at a downriver site (Fig. 1) every 2 h from 16:00 on June 12, 2011, until 22:00 on June 13, 2011. Additional four samples were collected at 9:35 on June 11, and at 9:00 and 12:00 on June 12, and at 14:47 on June 14, 2011 (Fig. 2). Compared to other CDOM samples before 20:00, June 12, the sample at 9:35, June 11 had an abnormally high light absorbance and was excluded due to possible contamination. The samples were filtered immediately through pre-combusted (at 500 °C for 5 h) GF/F filters for DOC and optical measurements. The filtrates were stored frozen for DOC measurements and refrigerated (4 °C) in the dark for optical measurements.

2.3. DOC and absorption measurements

The DOC concentration was measured by high temperature catalytic oxidation after removing dissolved inorganic C, by O_2 purging, using a Multi N/C 3100 TOC-TN analyzer (Analytik Jena, Germany, Hong et al., 2012). Each sample was measured in triplicate with a mean analytical precision of 1.4 ± 0.8%. A six-point calibration was carried out with solutions of potassium hydrogen phthalate as standards. The accuracy of the measurement was verified with Low Carbon Water and Deep Sea Water (from D. A. Hansell, University of Miami). The measured DOC concentration of Deep Sea Water (43.7 μmol L^{-1}) was in good agreement with the recommended values (44–46 μmol L^{-1}).

Absorbance spectra of CDOM were scanned with a Techcomp 2300 UV–Vis spectrometer at wavelengths 240–800 nm (every 1 nm) with Milli-Q water as the blank (Hong et al., 2012). Absorbance at each wavelength (λ) was baseline corrected by subtracting the mean absorbance at 700–800 nm, and converted to absorption coefficient ($a_{CDOM}(\lambda)$) as:

$$a_{CDOM}(\lambda) = 2.303 \times A(\lambda)/l \quad (1)$$

where $A(\lambda)$ is the corrected absorbance at wavelength λ and l is the path length (0.05 m). The absorption coefficient at 350 nm ($a_{CDOM}(350)$) is chosen to indicate the abundance of CDOM in this study. The carbon specific CDOM absorption coefficient at UV (λ = 254 nm), $SUVA_{254}$, was calculated as:

$$SUVA_{254} = a_{CDOM}(254)/DOC \quad (2)$$

$SUVA_{254}$ is correlated strongly to the aromaticity of DOM (Weishaar et al., 2003). The CDOM absorption spectral slope ratio (S_R), which is negatively correlated with the molecular weight of DOM, was calculated as the ratio of the spectral slope over 275–295 nm to that over 350–400 nm (Helms et al., 2008).

2.4. EEMs–PARAFAC

Sample fluorescence spectra (EEMs) were scanned using a Cary Eclipse fluorescence spectrophotometer (Varian, Australia) at emission wavelengths of 300–600 nm (every 2 nm), with excitation wavelengths of 250–450 nm (every 5 nm) (Hong et al., 2012). High absorption samples were diluted to $A(350) < 0.02$ at 1 cm pathlength before fluorescence measurements to avoid inner-filter effects (Moran et al., 2000; Kowalczuk et al., 2003). The spectra of each sample was calibrated with the Raman peak of Milli-Q water (Stedmon and Markager, 2005) and subtracted Raman-normalized spectra of Milli-Q water which was scanned on the same day.

All the 20 EEMs were subject to the multivariate modeling technique PARAFAC, using MATLAB 7.5 with "the N-way toolbox for MATLAB" (Stedmon and Bro, 2008). The low number of samples probably limited the number of fluorescent components identified using PARAFAC, but the PARAFAC model was validated by both the results of split-half analysis and the very low residuals. The number of components was determined with the split-half validation (Stedmon and Bro, 2008). One sample collected at 20:00 June 13 was identified as an outlier following the protocol of Stedmon and Bro (2008) and was, therefore, excluded from the PARAFAC model. EEMs were decomposed by PARAFAC into individual components with characteristic excitation–emission fluorescence spectra. Each component fluoresces over a series of excitation–emission wavelengths, and the maximum fluorescence of each component (F_{max}) was used to represent its fluorescence intensity in each sample (Stedmon and Markager, 2005; Kowalczuk et al., 2009; Hong et al., 2012). To examine changes in the composition of fluorescent DOM, the relative fraction of each component in the total fluorescence was also calculated (Kowalczuk et al., 2009; Yang et al., 2012b).

3. Results

3.1. Variation of DOC concentration and CDOM absorption

Overall, the DOC concentration increased from 1.7 mg L^{-1} in the pre-storm baseflow to 2.1 mg L^{-1} at stormflow and then decreased to ~1.8 mg L^{-1}, although there were some fluctuations (Fig. 3). There was a moderate correlation between the DOC concentration and the water discharge ($r = 0.60$, $p < 0.01$). These results agreed with the observation that the DOC concentration in the Jiulong River was higher after storms than in the dry season (Hong et al., 2012). The increase of DOC in the high-discharge stormflow was probably due to the changes in the hydrologic flowpath to the river from lower, mineral soil horizons during baseflow to upper soil and litter horizons during stormflow (Hood et al., 2006; Wiegner et al., 2009; Fellman et al., 2009; Spencer et al., 2010).

Values of $a_{CDOM}(350)$, $SUVA_{254}$ and S_R ranged within 3.10–6.53 m^{-1}, 6.07–10.24 $m^2 g^{-1}$, and 0.87–1.06, respectively (Fig. 3). The value of $a_{CDOM}(350)$ was generally low before 20:00, June 12 (3.10–3.41 m^{-1}), then increased rapidly to 6.27 m^{-1} at 18:00, June 13 and remained at relatively high levels. The elevation of $a_{CDOM}(350)$ in the storm event indicated that much more CDOM was flushed from the land into the river during the storm than during the baseflow condition. $SUVA_{254}$, which correlates positively to the aromaticity of DOM (Weishaar et al., 2003), showed a similar pattern of variation with $a_{CDOM}(350)$, suggesting an increase in the aromaticity of DOM in the storm event. S_R, which correlates negatively with the molecular weight of DOM (Helms et al., 2008), generally decreased during the study period though it varied little after 18:00, June 13, suggesting an increase in the molecular weight of DOM in the storm event.

3.2. Fluorescence components and variation of intensities

Generally, there are two types of fluorophores: humic-like and protein-like with maximum fluorescence at emission wavelengths $\geqslant$370 nm and approximately 340 and 305 nm, respectively (Coble, 2007; Mudarra et al., 2011). Three fluorescent components were identified using EEMs–PARAFAC in this study, including two humic-like (C1 and C3) and one combined (C2) component (Fig. 4). C1 had two excitation maxima at $\leqslant$250 and 335 nm and one emission maximum at 424 nm (Fig. 4A), similar to the humic-like C4 in Stedmon and Markager (2005) and C3 in Chen et al. (2010). C2, with excitation/emission maxima at 275/398 nm and a secondary peak at

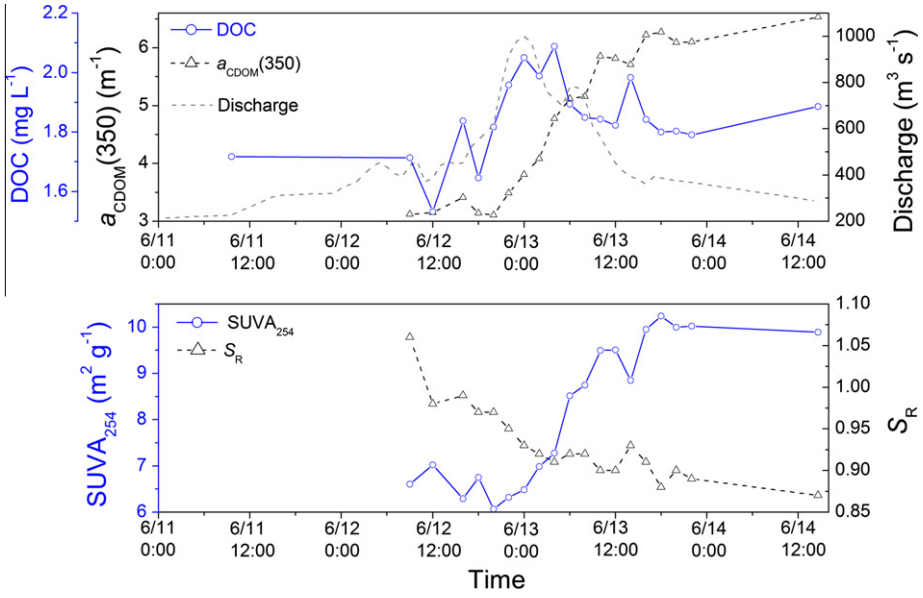

Fig. 3. Temporal changes in the DOC concentration, absorption coefficient of CDOM ($a_{CDOM}(350)$), carbon specific CDOM absorption coefficient at UV ($SUVA_{254}$) and spectral slope ratio (S_R).

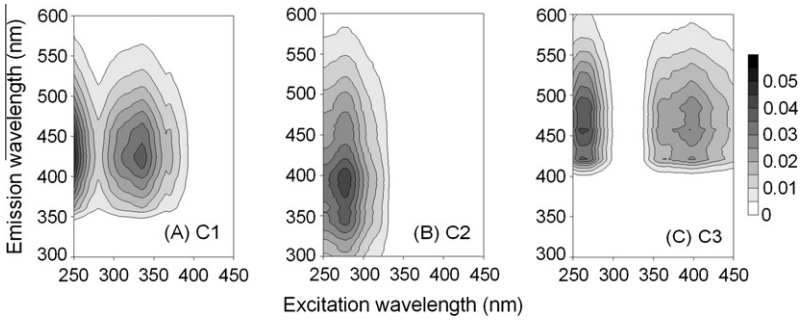

Fig. 4. Spectral characteristics of the three fluorescent components identified using parallel factor analysis.

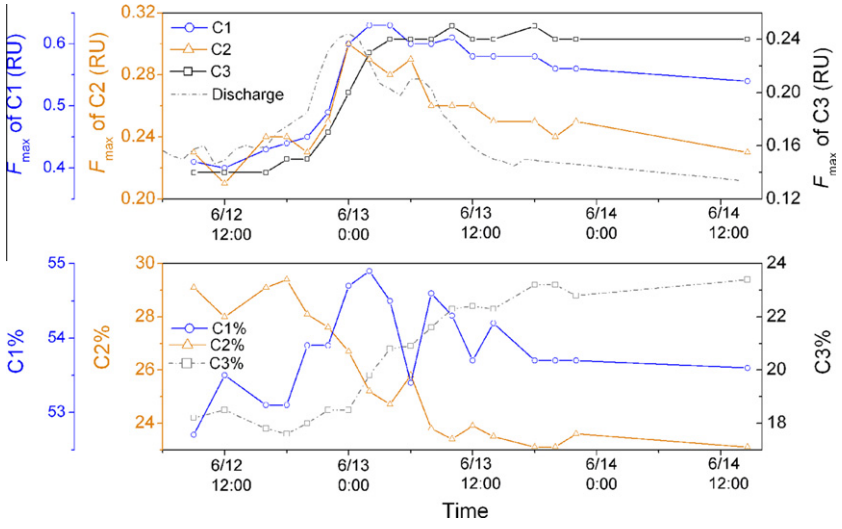

Fig. 5. Temporal changes in the fluorescence intensities of components C(1–3) and their fractions in the total fluorescence.

275/354 nm, covered the EEM spectral regions of both humic-like and tryptophan-like fluorophores (Fig. 4B, Coble, 2007; Mudarra et al., 2011). Therefore, C2 was a combined component containing both humic-like and protein-like DOM, similar to C2 in Yang et al. (2012a). C3, which had excitation/emission maxima at 260, 395/458 nm (Fig. 4C), resembled the humic-like C2 in Singh et al. (2010).

Table 1
Correlations between compositional proxies of DOM ($SUVA_{254}$: DOC-normalized absorption coefficient at 254 nm; S_R: absorption spectral slope ratio; C(1–3)%: fractions of C(1–3) in the total fluorescence).

	$SUVA_{254}$	S_R	C1%	C2%
S_R	−0.76***			
C1%	0.05	−0.50*		
C2%	−0.89***	0.88***	−0.48*	
C3%	0.97***	−0.83***	0.23	−0.97***

*** $p < 0.001$.
* $p < 0.05$.

Fluorescence intensities of the humic-like C1 and C3 were correlated strongly ($r = 0.92$, $p < 0.001$), which showed moderate correlations to that of C2 ($r = 0.79$, $p < 0.001$ and $r = 0.51$, $p < 0.05$, respectively). C1 and C3 were also correlated with $a_{CDOM}(350)$ ($r = 0.67$, $p < 0.001$ and $r = 0.90$, $p < 0.05$, respectively). C1 and C2 were correlated with DOC ($r = 0.70$, $p < 0.01$ and $r = 0.75$, $p < 0.001$, respectively). Fluorescence intensities of C(1–3) all showed notable increases during the rising limb of the stormflow hydrograph, indicating the flushing of fluorescent DOM into the river channel during the storm (Fig. 5). Thereafter, they showed different variations during the falling limb of the hydrograph, with the fluorescence intensity of C2 decreasing greatly and that of C3 remaining at relatively high values. There were also notable changes in the composition of fluorescent DOM. C2% generally decreased from 29.4% to 23.1% while C3% increased from 17.6% to 23.2% between 18:00, June 12 and 18:00, June 13 (Fig. 5). In fact, C2% and C3% showed a strong negative correlation ($r = -0.97$, Table 1). The C1% varied within a smaller range (52.7–54.9%) than C2% and C3%. The C1% increased during the rising-hydrograph of the stormflow, then decreased overall until 18:00, June 13 and remained constant thereafter.

4. Discussion

4.1. Influence of the summer storm event on the flux of DOM

Fluxes of DOC, CDOM and C(1–3) were calculated as the products of discharge ($m^3\ s^{-1}$) and DOC ($mg\ L^{-1}$), $a_{CDOM}(350)$ (m^{-1}) and F_{max} of C(1–3) (RU), respectively. The DOC concentration increased by 22% in the stormflow peak as compared to that at baseflow (Fig. 3). This, in combination with the increase in the water discharge during the storm event, led to an increase in the DOC flux by five times from 0.4 $kg\ s^{-1}$ at baseflow (at 9:35 June 11) to 2.0 $kg\ s^{-1}$ at peak flow (at 0:00 June 13) in the North Jiulong River. In fact, the DOC flux was strongly correlated with the water discharge ($r = 0.99$, $p < 0.0001$). For comparison, the DOC flux during stormflow can reach >10 times that at baseflow in both large rivers (e.g., Kyungan River, Nguyen et al., 2010) and small rivers (e.g., Wailuku River, Wiegner et al., 2009; McGinnis Creek and Peterson Creek, Fellman et al., 2009). The smaller increase in the DOC flux in the North Jiulong River than those in previous studies was mainly due to the smaller increase in the discharge. Many watershed characteristics could affect the magnitude of changes in the water discharge, the DOC concentration and the export of DOC in storm events, such as watershed size, slope, land cover, soil permeability and soil organic C content. Considering the important role of DOM in the cycles of C, nutrients and metals, the fivefold increase in the DOM flux in this study could influence many biogeochemical processes in the river and receiving coastal sea.

The contribution of storm events to the annual export of DOC in 2011 in the North Jiulong River was estimated roughly. The annual export flux of DOC was estimated by summing the daily flux of DOC. Seven storm events (with accumulated precipitation $\geqslant$50 mm in 24 h) were identified based on precipitation data and fluxes of DOC in stormflows were summed. Daily flux of DOC was estimated using two methods: (1) being retrieved from the regression equation between DOC flux (y, $kg\ s^{-1}$) and water discharge during the observation period (x, $m^3\ s^{-1}$) ($y = 0.00191x$, $r = 0.99$, $p < 0.0001$) using daily average water discharge; (2) being estimated as the product of daily average water discharge and DOC concentration, with DOC concentration being retrieved from the regression equation between DOC concentration (y, $mg\ L^{-1}$) and water discharge (x, $m^3\ s^{-1}$) during the observation period ($y = 0.000358x + 1.65$, $r = 0.60$, $p < 0.01$) using daily average water discharge. The result suggested that stormflows (2.7% of the time) contributed approximately 10% of the annual DOC export in 2011 in the North Jiulong River. The contribution of storm events to the annual export of DOC in the medium-sized North Jiulong River was smaller than those in small rivers (e.g., Kao and Liu, 1997; Buffam et al., 2001; Wiegner et al., 2009; Raymond and Saiers, 2010), due to smaller increases in the DOC flux during stormflows as mentioned above.

The fluxes of CDOM and fluorescent components were all correlated significantly with discharge ($r = 0.77$–0.99, $p < 0.001$) and showed large increases in the stormflow. This agreed with the case of Kyungan River (Nguyen et al., 2010). The increment in CDOM and fluorescent component fluxes in the stormwater may also be in part due to a cross-correlation between these parameters and DOC, which is commonly observed in aquatic environments (Asmala et al., 2012). Somewhat differently, in a Welsh peatland watershed, the levels of fluorescent components decreased due to dilution effects despite an increase in the CDOM level in storm events (Austnes et al., 2010). Overall, the present results indicated the influence of summer storm events on the export of DOM and its chromophoric and fluorescent constituents in the North Jiulong River.

In spite of the fact that the fluxes of DOC, CDOM and fluorescent components all increased with increasing discharge, there are also differences between their response to the storm event. The DOC flux was only slightly higher during the rising-hydrograph than during the falling-hydrograph of the stormflow at a given discharge (Fig. 6). The DOC flux was also greater during the falling-hydrograph than during the rising-hydrograph at equal discharge in a Welsh peatland watershed (Austnes et al., 2010) and a Korean agricultural-forested watershed (Nguyen et al., 2010) (calculated from their flow and DOC concentration data). Small-forested watersheds in the eastern USA showed the opposite trend, where the DOC concentration (and the DOC flux) during the rising-hydrograph are greater than those during the falling-hydrograph at equal discharge (Buffam et al., 2001; Raymond and Saiers, 2010). Therefore, although the DOC flux increases during the stormflow, whether it is dominated by flushing or dilution effect during the falling-hydrograph varies in different studies. This is probably in part associated with differences in the flushing ability of storm events (e.g., the precipitation), various terrestrial organic matter pools, watershed area, land cover, geomorphology and soil permeability, etc. For example, with a greater storm flushing and a smaller pool size of terrestrial DOM, it is more probable that the dilution effect dominates during the falling-hydrograph. On a longer time scale, the DOM level is much lower during post-flush periods than during flush periods in a tropical rainforest river (Spencer et al., 2010). In addition, if there is a near-stream or in-stream source of DOM during storms (e.g., the riparian zone), the concentration and the flux of DOM might increase rapidly during the rising-hydrograph of stormflow, leading to a clockwise hysteresis loop in the flux–discharge graph (Buffam et al., 2001; Hood et al., 2006).

In contrast to the small difference between DOC fluxes during the rising and falling hydrographs, fluxes of CDOM and fluorescent components during the falling-hydrograph were higher than those

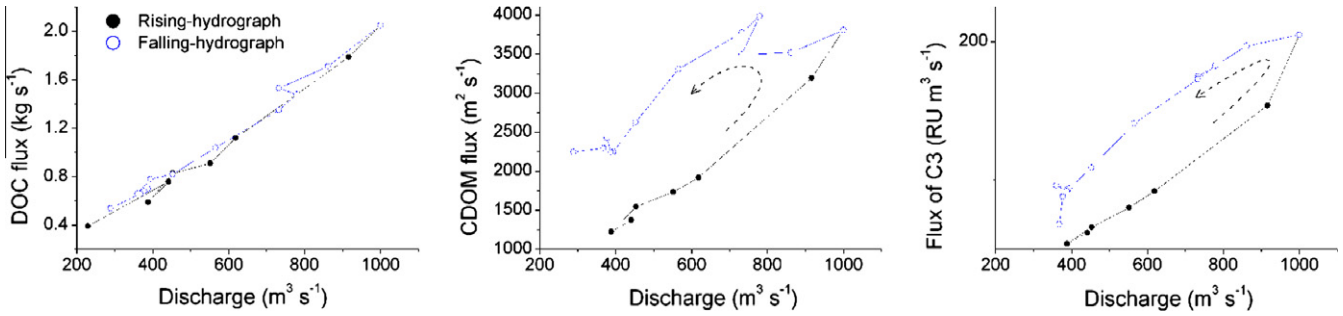

Fig. 6. Flux–discharge graphs of DOC, CDOM and C3 during the study period (flux–discharge graphs of C(1–2) were similar to that of C3).

during the rising-hydrograph at equal discharge, showing evident counterclockwise hysteresis loops in the flux–discharge graph (Fig. 6). This resulted from that CDOM and fluorescent components (especially C1 and C3) remained at high levels during the falling-hydrograph. Similarly, the CDOM level remained at high levels for several days after a storm event in a peatland watershed (Event 3 in Austnes et al., 2010). The enhanced light-absorption by CDOM in the storm event would increase the light attenuation in the water column and decrease the aquatic primary production, which may also be decreased by the increasing suspended sediment load and the reducing water residence time but be increased by elevated nutrient level in the storm event.

4.2. Influence of the summer storm event on the composition of DOM

Since humic-rich terrestrial organic matter was flushed into the river channel and bulk DOC, CDOM and fluorescent components exhibited different dynamics, it was reasonable that there was a notable change in the river DOM composition in the storm event. On one hand, the increase in $SUVA_{254}$ and the decrease in S_R suggested an increase in the aromaticity and molecular weight of DOM in the storm event (Fig. 3; Weishaar et al., 2003; Helms et al., 2008). On the other hand, after the flow peak, CDOM, C1 and C3 remained at elevated levels while the level of C2 decreased notably. The fraction of C3 which emitted fluorescence at longer emission wavelengths increased, while that of C2 (including protein-like DOM) which fluoresced at shorter emission wavelengths decreased (Fig. 5). There were strong correlations between $SUVA_{254}$, S_R, and C(2–3)% (Table 1). The positive correlation between S_R and C2% also suggested that the combined component was likely to have a lower average molecular weight than the humic-like components. Similarly, Nguyen et al. (2010) revealed that the protein-like fraction in synchronous fluorescence correlated negatively with the average molecular weight determined by size exclusion chromatography. Huguet et al. (2010) reported that the protein-like fluorescence occurred in the low molecular size fraction (<1 kDa) separated with ultra-filtration.

Changes in the level and composition of DOM in the North Jiulong River during the storm event were probably associated shifts in inputs of DOM from various sources. Under the baseflow condition, the flowpath of DOM from the land to the river was mainly through the groundwater discharge in the lower, organic-poor mineral soil horizons, limiting the input of terrestrial DOM. The proportion of autochthonous DOM was higher in the baseflow than in the stormflow, which generally had lower molecular weight and aromaticity but a higher percentage of protein-like fluorophores than terrestrial DOM (Yamashita et al., 2010; Hong et al., 2012). Therefore, the DOC concentration, $a_{CDOM}(350)$, fluorescence intensities of C(1–3), $SUVA_{254}$, C1% and C3% were lower but S_R and C2% were higher in the baseflow than in the stormflow (Figs. 3 and 5).

Under the stormflow condition, surface runoff through the organic-rich upper soil and litter horizons in both the riparian zone and upper hillslopes increased greatly, enhancing the flow of allochthonous DOM into the river. DOM from the riparian zone (including wetlands, residential areas and agricultural lands) was flushed into the river most rapidly. Surface runoff from forested hillslopes also rapidly transported DOM (which originated from leaching of plants by throughfall and leaching of surface soil and litter) into the river. The inflow of DOM from those riparian and surface sources probably led to increases in the DOC concentration, $a_{CDOM}(350)$, fluorescence intensities of C(1–3), $SUVA_{254}$, C1% and C3% but decreases in S_R and C2% from the baseflow to the flow peak (Figs. 3 and 5). In particular, DOM from residential areas contained abundant protein-like fluorophores and could explain in part the increase in the fluorescence intensity of C2 (Yang et al., 2012b). Rainfall and leachate of plants might also contain C2 (Ohno and Bro, 2006; Kieber et al., 2007). Wetlands probably contributed more humic-like materials (Hood et al., 2006; Fellman et al., 2009; Williams et al., 2010). DOM from the leaching of plants, surface soil and litter were likely fresh and less humified, which could explain increases in the fluorescence intensity of C1 and C1%. The C1 fluoresced at shorter emission wavelengths than C3 and was likely less aromatic/humified.

After the rapid flushing, the contribution of DOM from riparian and surface sources decreased while that from deeper humified soil organic matter in forestlands increased. The more humified DOM was leached and carried by waters penetrating into the soil and flowing out more slowly than surface runoff. This DOM from forest soils was dominated by condensed, high molecular weight humic materials with strong light absorption (Yamashita et al., 2011; Yang et al., 2012b). Therefore, although the DOC concentration and fluorescence intensity of C2 decreased after the flow peak, $a_{CDOM}(350)$, fluorescence intensities of humic-like C1 and C3, $SUVA_{254}$ and C3% remained at high levels while S_R and C2% was low (Figs. 3 and 5). The C1% also showed an overall decreasing trend after the flow peak since the more humified C3 was probably more abundant than C1 in the humified layer of forest soils.

How the composition changed with the flux was examined for CDOM and fluorescent components (Fig. 7). The S_R-CDOM flux graph showed an overall clockwise hysteresis loop, suggesting that DOM had a higher average molecular weight (and also a higher aromaticity, considering the correlation between $SUVA_{254}$ and S_R) during the falling-hydrograph than during the rising-hydrograph at equal CDOM flux. This was mainly due to the decrease in S_R lagged behind discharge, since S_R generally decreased with increasing $a_{CDOM}(350)$ and showed no hysteresis loop with $a_{CDOM}(350)$. In addition, C2% was lower during the falling-hydrograph than during the rising-hydrograph at equal flux of C2. This was associated with the decrease in C2% lagged behind both discharge and F_{max} of C2. Overall, the changes in the composition lagged behind those in the flux of DOM and could last after the water discharge had decreased, indicating the important influence of the storm event on the DOM composition.

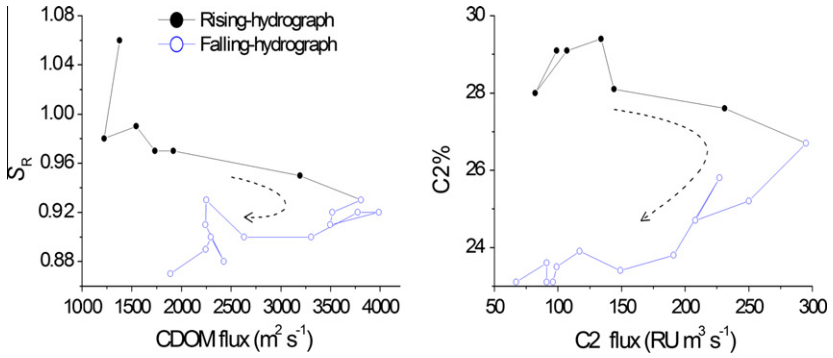

Fig. 7. Typical graphs of compositional proxy vs. flux for CDOM and fluorescent components in the storm event (note significant correlations for $SUVA_{254}$ vs. S_R, C3% vs. C2% (Table 1) and fluxes of C1 and C3 vs. flux of C2 ($r = 0.98–0.93$, $p < 0.001$)).

The biogeochemical reactivity of DOM is largely determined by its chemical composition. For example, several studies illustrate a positive correlation between the bioavailability and the protein-like fraction of DOM (e.g., Fellman et al., 2009, 2010). In contrast, humic-like DOM is probably more susceptible to photochemical degradation (Kieber et al., 2007; Spencer et al., 2009). The compositional change of DOM in the storm event would affect its biogeochemical role in the Jiulong River and the receiving estuarine and coastal waters.

5. Conclusions

Both the flux and composition of DOM showed notable changes during a summer storm event in the subtropical Jiulong River. A significant increase in the flux of DOC, CDOM and fluorescent components during the storm event indicated the substantial impact of the storm event on the export of DOM and its chromophoric and fluorescent constituents. Stormflows (<3% of the time) could contribute ~10% of the annual DOC export. The flux–discharge graphs of DOC, CDOM and fluorescent components were different. The flux of DOC was only slightly higher during the rising-hydrograph than during the falling-hydrograph of the stormflow at equal water discharge, while those of CDOM and fluorescent components (in particular, humic-like C1 and C3) were elevated notably in the falling-hydrograph. Such differences in the transport and behavior of DOM and its components might be associated with inputs of various DOM sources in the watershed. An increase in $SUVA_{254}$ accompanied with a decrease in S_R suggested a notable increase in the aromaticity and average molecular weight of DOM in the storm event. The fraction of C3 which emitted fluorescence at longer emission wavelengths increased, while that of C2 (including protein-like DOM) decreased. These four compositional proxies correlated to each other and were probably affected strongly by the enhanced inflow of terrestrial organic matter during the storm event. The results showed that changes in the flux and chemical composition of DOM during storm events could be monitored effectively by absorption spectroscopy and EEMs–PARAFAC at high temporal resolution. The export of DOM via storm runoff is expected to affect biogeochemical processes in the Jiulong River and the receiving coastal waters. Therefore, although storms are relatively short-lived events, they have significant ramifications for the biogeochemistry of receiving waters.

Acknowledgements

This study was supported by the Fundamental Research Funds for the Central Universities (No. 201112G011), the National Natural Science Foundation of China (Nos. 40810069004, 41276064 and 40776041) and the MEL Young Scientist Visiting Fellowship of State Key Lab of Marine Environmental Science (Xiamen University). We thank Jiezhong Wu for assistance in sampling, and Haiping Shen from Punan Gauge for providing flow data during the storm event. Dr. Robert G.M. Spencer is appreciated greatly for constructive comments and help in English. Dr. Rudolf Jaffé and Dr. Piotr Kowalczuk are thanked for their comments that greatly improved the quality of the paper.

References

Asmala, E., Stedmon, C.A., Thomas, D.N., 2012. Linking CDOM spectral absorption to dissolved organic carbon concentrations and loadings in boreal estuaries. Estuar. Coast. Shelf Sci. 111, 107–117.

Austnes, K., Evans, C.D., Eliot-Laize, C., Naden, P.S., Old, G.H., 2010. Effects of storm events on mobilisation and in-stream processing of dissolved organic matter (DOM) in a Welsh peatland catchment. Biogeochemistry 99, 157–173.

Battin, T.J., Kaplan, L.A., Findlay, S., Hopkinson, C.S., Marti, E., Packman, A.I., Newbold, J.D., Sabater, F., 2008. Biophysical controls on organic carbon fluxes in fluvial networks. Nat. Geosci. 1, 95–100.

Benner, R., 2003. Molecular indicators of the bioavailability of dissolved organic matter. In: Findlay, S., Sinsabaugh, R.L. (Eds.), Aquatic Ecosystems: Interactivity of Dissolved Organic Matter. Academic Press, New York, pp. 121–137.

Buffam, I., Galloway, J.N., Blum, L.K., McGlathery, K.J., 2001. A stormflow/baseflow comparison of dissolved organic matter concentrations and bioavailability in an Appalachian stream. Biogeochemistry 53, 269–306.

Cawley, K., Wolski, P., Mladenov, N., Jaffé, R., 2012. Dissolved organic matter biogeochemistry along a transect of the Okavango Delta, Botswana. Wetlands. http://dx.doi.org/10.1007/s13157-012-0281-0.

Chen, M.L., Price, R.M., Yamashita, Y., Jaffe, R., 2010. Comparative study of dissolved organic matter from groundwater and surface water in the Florida coastal Everglades using multi-dimensional spectrofluorometry combined with multivariate statistics. Appl. Geochem. 25, 872–880.

Coble, P.G., 2007. Marine optical biogeochemistry: the chemistry of ocean color. Chem. Rev. 107, 402–418.

Fellman, J.B., Hood, E., Edwards, R.T., D'Amore, D.V., 2009. Changes in the concentration, biodegradability, and fluorescent properties of dissolved organic matter during stormflows in coastal temperate watersheds. J. Geophys. Res. 114, G01021, doi: http://dx.doi.org/01010.01029/02008JG000790.

Fellman, J.B., Hood, E., Spencer, R.G.M., 2010. Fluorescence spectroscopy opens new windows into dissolved organic matter dynamics in freshwater ecosystems: a review. Limnol. Oceanogr. 55, 2452–2462.

Hassler, C.S., Schoemann, V., Nichols, C.M., Butler, E.C.V., Boyd, P.W., 2011. Saccharides enhance iron bioavailability to Southern Ocean phytoplankton. Proc. Natl. Acad. Sci. USA 108, 1076–1081.

He, B.Y., Dai, M.H., Zhai, W.D., Wang, L.F., Wang, K.J., Chen, J.H., Lin, J.R., Han, A.G., Xu, Y.P., 2010. Distribution, degradation and dynamics of dissolved organic carbon and its major compound classes in the Pearl River estuary, China. Mar. Chem. 119, 52–64.

Helms, J.R., Stubbins, A., Ritchie, J.D., Minor, E.C., Kieber, D.J., Mopper, K., 2008. Absorption spectral slopes and slope ratios as indicators of molecular weight, source, and photobleaching of chromophoric dissolved organic matter. Limnol. Oceanogr. 53, 955–969.

Hong, H.S., Yang, L.Y., Guo, W.D., Wang, F.L., Yu, X.X., 2012. Characterization of dissolved organic matter under contrasting hydrologic regimes in a subtropical watershed using PARAFAC model. Biogeochemistry 109, 163–174.

Hood, E., Gooseff, M.N., Johnson, S.L., 2006. Changes in the character of stream water dissolved organic carbon during flushing in three small watersheds, Oregon. J. Geophys. Res. 111, G01007. http://dx.doi.org/10.1029/2005JG000082.

Huang, J.L., Li, Q.S., Hong, H.S., Lin, J., Qu, M.C., 2011. Preliminary study on linking land use & landscape pattern and water quality in the Jiulong River Watershed. Environ. Sci. 32, 64–72 (in Chinese with English abstract).

Huguet, A., Vacher, L., Saubusse, S., Etcheber, H., Abril, G., Relexans, S., Ibalot, F., Parlanti, E., 2010. New insights into the size distribution of fluorescent dissolved organic matter in estuarine waters. Org. Geochem. 41, 595–610.

IPCC, 2007. Climate Change 2007: Synthesis Report. Contribution of Working Groups I, II and III to the Fourth Assessment Report of the Intergovernmental Panel on Climate Change, Geneva.

Jiao, N., Herndl, G.J., Hansell, D.A., Benner, R., Kattner, G., Wilhelm, S.W., Kirchman, D.L., Weinbauer, M.G., Luo, T., Chen, F., Azam, F., 2010. Microbial production of recalcitrant dissolved organic matter: long-term carbon storage in the global ocean. Nat. Rev. Microbiol. 8, 593–599.

Kao, S.J., Liu, K.K., 1997. Fluxes of dissolved and nonfossil particulate organic carbon from an Oceania small river (Lanyang Hsi) in Taiwan. Biogeochemistry 39, 255–269.

Kieber, R.J., Willey, J.D., Whitehead, R.F., Reid, S.N., 2007. Photobleaching of chromophoric dissolved organic matter (CDOM) in rainwater. J. Atmos. Chem. 58, 219–235.

Kowalczuk, P., Cooper, W.J., Whitehead, R.F., Durako, M.J., Sheldon, W., 2003. Characterization of CDOM in an organic-rich river and surrounding coastal ocean in the South Atlantic Bight. Aquat. Sci. 65, 384–401.

Kowalczuk, P., Durako, M.J., Young, H., Kahn, A.E., Cooper, W.J., Gonsior, M., 2009. Characterization of dissolved organic matter fluorescence in the South Atlantic Bight with use of PARAFAC model: interannual variability. Mar. Chem. 113, 182–196.

Loh, A.N., Bauer, J.E., Druffel, E.R.M., 2004. Variable ageing and storage of dissolved organic components in the open ocean. Nature 430, 877–881.

Lonborg, C., Sondergaard, M., 2009. Microbial availability and degradation of dissolved organic carbon and nitrogen in two coastal areas. Estuar. Coast. Shelf Sci. 81, 513–520.

Ludwig, W., Probst, J.L., Kempe, S., 1996. Predicting the oceanic input of organic carbon by continental erosion. Global Biogeochem. Cycles 10, 23–41.

Maie, N., Yamashita, Y., Cory, R.M., Boyer, J.N., Jaffé, R., 2012. Application of excitation emission matrix fluorescence monitoring in the assessment of spatial and seasonal drivers of dissolved organic matter composition: sources and physical disturbance controls. Appl. Geochem. 27, 917–929.

Mayorga, E., Aufdenkampe, A.K., Masiello, C.A., Krusche, A.V., Hedges, J.I., Quay, P.D., Richey, J.E., Brown, T.A., 2005. Young organic matter as a source of carbon dioxide outgassing from Amazonian rivers. Nature 436, 538–541.

Moran, M.A., Zepp, R.G., 1997. Role of photoreactions in the formation of biologically labile compounds from dissolved organic matter. Limnol. Oceanogr. 42, 1307–1316.

Moran, M.A., Sheldon, W.M., Zepp, R.G., 2000. Carbon loss and optical property changes during long-term photochemical and biological degradation of estuarine dissolved organic matter. Limnol. Oceanogr. 45, 1254–1264.

Mudarra, M., Andreo, B., Baker, A., 2011. Characterisation of dissolved organic matter in karst spring waters using intrinsic fluorescence: relationship with infiltration processes. Sci. Total Environ. 409, 3448–3462.

Nguyen, H., Hur, J., Shin, H.-S., 2010. Changes in spectroscopic and molecular weight characteristics of dissolved organic matter in a river during a storm event. Water Air Soil Pollut. 212, 395–406.

Ohno, T., Bro, R., 2006. Dissolved organic matter characterization using multiway spectral decomposition of fluorescence landscapes. Soil Sci. Soc. Am. J. 70, 2028–2037.

Raymond, P.A., Saiers, J.E., 2010. Event controlled DOC export from forested watersheds. Biogeochemistry 100, 197–209.

Sánchez-Marín, P., Santos-Echeandía, J., Nieto-Cid, M., Álvarez-Salgado, X.A., Beiras, R., 2010. Effect of dissolved organic matter (DOM) of contrasting origins on Cu and Pb speciation and toxicity to *Paracentrotus lividus* larvae. Aquat. Toxicol. 96, 90–102.

Singh, S., D'Sa, E.J., Swenson, E.M., 2010. Chromophoric dissolved organic matter (CDOM) variability in Barataria Basin using excitation–emission matrix (EEM) fluorescence and parallel factor analysis (PARAFAC). Sci. Total Environ. 408, 3211–3222.

Spencer, R.G.M., Stubbins, A., Hernes, P.J., Baker, A., Mopper, K., Aufdenkampe, A.K., Dyda, R.Y., Mwamba, V.L., Mangangu, A.M., Wabakanghanzi, J.N., Six, J., 2009. Photochemical degradation of dissolved organic matter and dissolved lignin phenols from the Congo River. J. Geophys. Res. 114, G03010, doi: http://dx.doi.org/03010.01029/02009JG000968.

Spencer, R.G.M., Hernes, P.J., Ruf, R., Baker, A., Dyda, R.Y., Stubbins, A., Six, J., 2010. Temporal controls on dissolved organic matter and lignin biogeochemistry in a pristine tropical river, Democratic Republic of Congo. J. Geophys. Res. 115, G03013, doi: http://dx.doi.org/03010.01029/02009JG001180.

Stedmon, C.A., Bro, R., 2008. Characterizing dissolved organic matter fluorescence with parallel factor analysis: a tutorial. Limnol. Oceanogr. – Method 6, 572–579.

Stedmon, C.A., Markager, S., 2005. Resolving the variability in dissolved organic matter fluorescence in a temperate estuary and its catchment using PARAFAC analysis. Limnol. Oceanogr. 50, 686–697.

Stedmon, C.A., Markager, S., Tranvik, L., Kronberg, L., Slatis, T., Martinsen, W., 2007. Photochemical production of ammonium and transformation of dissolved organic matter in the Baltic Sea. Mar. Chem. 104, 227–240.

Stubbins, A., Spencer, R.G.M., Chen, H.M., Hatcher, P.G., Mopper, K., Hernes, P.J., Mwamba, V.L., Mangangu, A.M., Wabakanghanzi, J.N., Six, J., 2010. Illuminated darkness: molecular signatures of Congo River dissolved organic matter and its photochemical alteration as revealed by ultrahigh precision mass spectrometry. Limnol. Oceanogr. 55, 1467–1477.

Weishaar, J.L., Aiken, G.R., Bergamaschi, B.A., Fram, M.S., Fujii, R., Mopper, K., 2003. Evaluation of specific ultraviolet absorbance as an indicator of the chemical composition and reactivity of dissolved organic carbon. Environ. Sci. Technol. 37, 4702–4708.

Wiegner, T.N., Tubal, R.L., MacKenzie, R.A., 2009. Bioavailability and export of dissolved organic matter from a tropical river during base- and stormflow conditions. Limnol. Oceanogr. 54, 1233–1242.

Williams, C.J., Yamashita, Y., Wilson, H.F., Jaffe, R., Xenopoulos, M.A., 2010. Unraveling the role of land use and microbial activity in shaping dissolved organic matter characteristics in stream ecosystems. Limnol. Oceanogr. 55, 1159–1171.

Yamashita, Y., Maie, N., Briceno, H., Jaffe, R., 2010. Optical characterization of dissolved organic matter in tropical rivers of the Guayana Shield, Venezuela. J. Geophys. Res. 115, G00F10. http://dx.doi.org/10.1029/2009JG000987.

Yamashita, Y., Kloeppel, B., Knoepp, J., Zausen, G., Jaffé, R., 2011. Effects of watershed history on dissolved organic matter characteristics in headwater streams. Ecosystems 14, 1110–1122.

Yang, L.Y., Hong, H.S., Guo, W.D., Chen, C.-T.A., Pan, P.-I., Feng, C.-C., 2012a. Absorption and fluorescence of dissolved organic matter in submarine hydrothermal vents off NE Taiwan. Mar. Chem. 128–129, 64–71.

Yang, L.Y., Hong, H.S., Guo, W.D., Huang, J.L., Li, Q.S., Yu, X.X., 2012b. Effects of changing land use on dissolved organic matter in a subtropical river watershed, southeast China. Reg. Environ. Change 12, 145–151.